AD

USAAVLABS TECHNICAL REPORT 69-65

BUCKLING OF ELECTROFORMED CONICAL SHELLS UNDER HYDROSTATIC PRESSURE

By

Josef Singer
Dror Bendavid

September 1971

EUSTIS DIRECTORATE
U. S. ARMY AIR MOBILITY RESEARCH AND DEVELOPMENT LABORATORY
FORT EUSTIS, VIRGINIA

CONTRACT DAAJ02-67-C-0031
STANFORD UNIVERSITY
STANFORD, CALIFORNIA

DISCLAIMERS

The findings in this report are not to be construed as an official Department of the Army position unless so designated by other authorized documents.

When Government drawings, specifications, or other data are used for any purpose other than in connection with a definitely related Government procurement operation, the United States Government thereby incurs no responsibility nor any obligation whatsoever; and the fact that the Government may have formulated, furnished, or in any way supplied the said drawings, specifications, or other data is not to be regarded by implication or otherwise as in any manner licensing the holder or any other person or corporation, or conveying any rights or permission, to manufacture, use, or sell any patented invention that may in any way be related thereto.

Trade names cited in this report do not constitute an official endorsement or approval of the use of such commercial hardware or software.

DISPOSITION INSTRUCTIONS

Destroy this report when no longer needed. Do not return it to the originator.

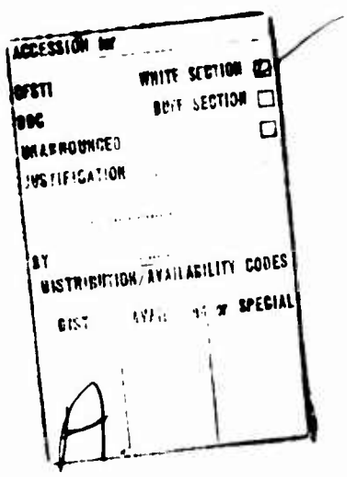

UNCLASSIFIED

Security Classification

DOCUMENT CONTROL DATA - R & D

(Security classification of title, body of abstract and indexing annotation must be entered when the overall report is classified)

1 ORIGINATING ACTIVITY (Corporate author) Stanford University Stanford, Calif.	2a. REPORT SECURITY CLASSIFICATION Unclassified 2b. GROUP

3 REPORT TITLE

BUCKLING OF ELECTROFORMED CONICAL SHELLS UNDER HYDROSTATIC PRESSURE

4 DESCRIPTIVE NOTES (Type of report and inclusive dates)

5 AUTHOR(S) (First name, middle initial, last name)

Josef Singer
Dror Bendavid

6 REPORT DATE	7a. TOTAL NO. OF PAGES	7b. NO. OF REFS
September 1971	48	20

8a. CONTRACT OR GRANT NO	9a. ORIGINATOR'S REPORT NUMBER(S)
DAAJ02-67-C-0031 b. PROJECT NO. Task 1F162204A17002 c. d.	USAAVLABS Technical Report 69-65 9b. OTHER REPORT NO(S) (Any other numbers that may be assigned this report)

10 DISTRIBUTION STATEMENT

Approved for public release; distribution unlimited.

11 SUPPLEMENTARY NOTES	12 SPONSORING MILITARY ACTIVITY
	Eustis Directorate, U.S. Army Air Mobility Research and Development Laboratory Fort Eustis, Virginia

13 ABSTRACT

The report describes a series of tests made on the buckling of high quality electroformed conical shells under hydrostatic pressure. The thirteen shells used were all of high taper ratio, ten having a taper ratio of 0.75 and 3 are of 0.669. The range of average radius to wall thickness covered was from 600-1200. The method of testing is discussed in detail, and the results obtained are compared with the linear theories of Seide and Singer.

DD FORM 1 NOV 68 1473

UNCLASSIFIED

Security Classification

14. KEY WORDS	LINK A		LINK B		LINK C	
	ROLE	WT	ROLE	WT	ROLE	WT
Buckling						
Instability						
Conical Shells						
Linear Theory of Conical Shells						
Thin Walled Conical Shells						

DEPARTMENT OF THE ARMY
U. S. ARMY AIR MOBILITY RESEARCH & DEVELOPMENT LABORATORY
EUSTIS DIRECTORATE
FORT EUSTIS, VIRGINIA 23604

This program was carried out under Contract DAAJ02-67-C-0031 with Stanford University.

The data contained in this report are the result of research conducted to investigate the instability of thin, truncated conical shells of large taper ratios under hydrostatic pressure and the correlation of experimental results with linear theory.

The report has been reviewed by this Directorate and is considered to be technically sound. It is published for the exchange of information and the stimulation of future research.

This program was conducted under the technical management of Mr. James P. Waller, Structures Division.

Task 1F162204A17002
Contract DAAJ02-67-C-0031
USAAVLABS Technical Report 69-65
September 1971

BUCKLING OF ELECTROFORMED CONICAL SHELLS UNDER HYDROSTATIC PRESSURE

by

Josef Singer
Dror Bendavid

Prepared by

Stanford University
Department of Aeronautics and Astronautics
Stanford, California

for

EUSTIS DIRECTORATE
U.S. ARMY AIR MOBILITY RESEARCH AND DEVELOPMENT LABORATORY
FORT EUSTIS, VIRGINIA

ABSTRACT

The results of an experimental investigation of the instability of thin, truncated conical shells of large taper ratio under hydrostatic pressure are discussed and correlated with theory. The specimens were nickel shells produced by electroforming. The test results remove any doubts about the validity of the theories of Seide and Singer for cones of large taper ratio. Typical experimental results are also compared with a more recent theory that includes in-plane boundary condition effects.

FOREWORD

The authors wish to express their gratitude to Professor W. H. Horton and Mr. R. W. Johnson of Stanford University and to Mr. T. Weller of the Technion for helpful discussions and assistance in the test program.

The work reported herein was authorized by Contract DAAJ02-67-C-0031, Task 1F162204A17002.

BLANK PAGE

TABLE OF CONTENTS

LIST OF ILLUSTRATIONS

LIST OF TABLES

LIST OF SYMBOLS

a	distance of the top of a truncated cone from the vertex along a generator (see Figure 1)
E	modulus of elasticity
ε	$p/\bar{p}$, correlation function
h	thickness of shell
ℓ	slant length of cone
$M_x, N_x, N_{x\varphi}$	additional moment and forces caused by buckling
p_{cr}	experimental pressure
p_{th}	theoretical critical pressure[11]
p_1, p_2	theoretical critical pressure taking into account in-plane boundary conditions[18], for $E = 28 \times 10^6$ psi
$\bar{p}$	critical pressure of equivalent cylindrical shell
R_1	radius of small end of truncated cone
R_2	radius of large end of truncated cone
t	number of circumferential waves
u^*, v^*, w^*	displacements
u, v, w	nondimensional displacements, $u=(u^*/a)$, $v=(v^*/a)$, $w=(w^*/a)$
x^*	axial coordinate along a generator
x	nondimensional axial coordinate, $x=(x^*/a)$
x_2	ratio of the distance of the bottom of a truncated cone from the vertex to that of the top
α	cone angle
ξ	$x-1$
ν	Poisson's ratio
ρ_{av}	mean radius of curvature = $(R_1 + R_2)/2 \cos \alpha$
φ	circumferential coordinate
Ψ	taper ratio = $\frac{R_1}{R_2}$

INTRODUCTION

Experimental results for buckling of conical shells under hydrostatic pressure (see References 1 through 7) agree fairly well with linear theory, though they show considerable scatter. The scatter is of the same order as that obtained in recent tests of cylindrical shells of high (R/h) ratios,[4,8] whereas the older tests of cylindrical shells which fitted the linear theory so neatly - for example, Figure 6 of Reference 9 - were for specimens of small (R/h) ratios. Weingarten and Seide[4] pointed out that the discrepancy between experiment and theory is larger for conical shells of high taper ratio than for cylindrical shells. When the theoretical critical pressures of conical shells are correlated with those of equivalent cylindrical shells,[10,11] a correlation curve (or a family of correlation curves if one considers large cone angles[12]) is obtained which has a "hump" at large taper ratios. Weingarten and Seide[4] concluded that experiments do not verify this "hump". However, careful analysis of the results obtained in References 1 and 2 showed a trend to confirm the "hump", if the partial clamping of edges was taken into consideration.

The aim of the present experimental investigation is to settle this point more conclusively. The technique of manufacturing accurate nickel shells by electroforming developed at Stanford University[13] was utilized, and after further development, very thin conical shells of high uniformity were prepared. All the specimens had fairly high taper ratios in order to be in range of the "hump" in the correlation curve. The results confirm the validity of the linear theories[10,11] in the "hump" region.

TEST APPARATUS

SIMULATION OF THE BOUNDARY CONDITIONS

In attempting to set up an experimental investigation, the results of which are to be correlated with theory, one must seek to experimentally approach the theoretical boundary conditions as closely as possible.

For the case of a truncated conical shell, the boundary conditions referred to as simple supports are defined in most cases (for example, see Reference 11, 14, 15, and 16) as

Zero radial displacement	$w = 0$	
Zero circumferential displacement	$v = 0$	
No restraint in the direction of the generators	$u \neq 0, \ (N_x = 0)$	(1)
Free rotation of generators at the ends $x = 1$ and $x = x_2$	$w_{,xx} - (\nu/x)w_{,x} = 0$	

Another definition of simple supports for conical shells given by Seide[10] replaces $w = 0$ by the zero displacement normal to the cone axis:

$$w \cos \alpha - u \sin \alpha = 0 \qquad (2)$$

These boundary conditions offer slightly less resistance to buckling under external pressure than those given by equation (1); however, the actual effect of this difference on the buckling pressure is rather small, since u is of a smaller order of magnitude than w.

In the test rig, the uniform pressure on the external surface of the cone was produced by pumping air out of the test specimen. Therefore, it was necessary to design the boundary supports to serve as a good approximation to the theoretical boundary conditions while at the same time provide adequate sealing of the system under partial vacuum.

Supports with circular profiles (as used in Reference 1) that permit a certain amount of rotational freedom for the generators were therefore adopted. The inner support discs are provided with O-seals which fit exactly into carefully designed grooves at the contact lines (see Figure 2). The O-seal materials and sectional diameters were selected to be flexible enough to provide adequate sealing, yet to maintain enough rigidity so as not to impair rotation of the generators.

Displacement along the generators is restrained by the friction of the O-seals and outer support rings (Figure 2, parts no. 10 and 19); but axial movement of the ends as a whole is not restricted.

Though it has recently been shown that axial restraint may significantly increase the buckling pressure for cylindrical and conical shells under

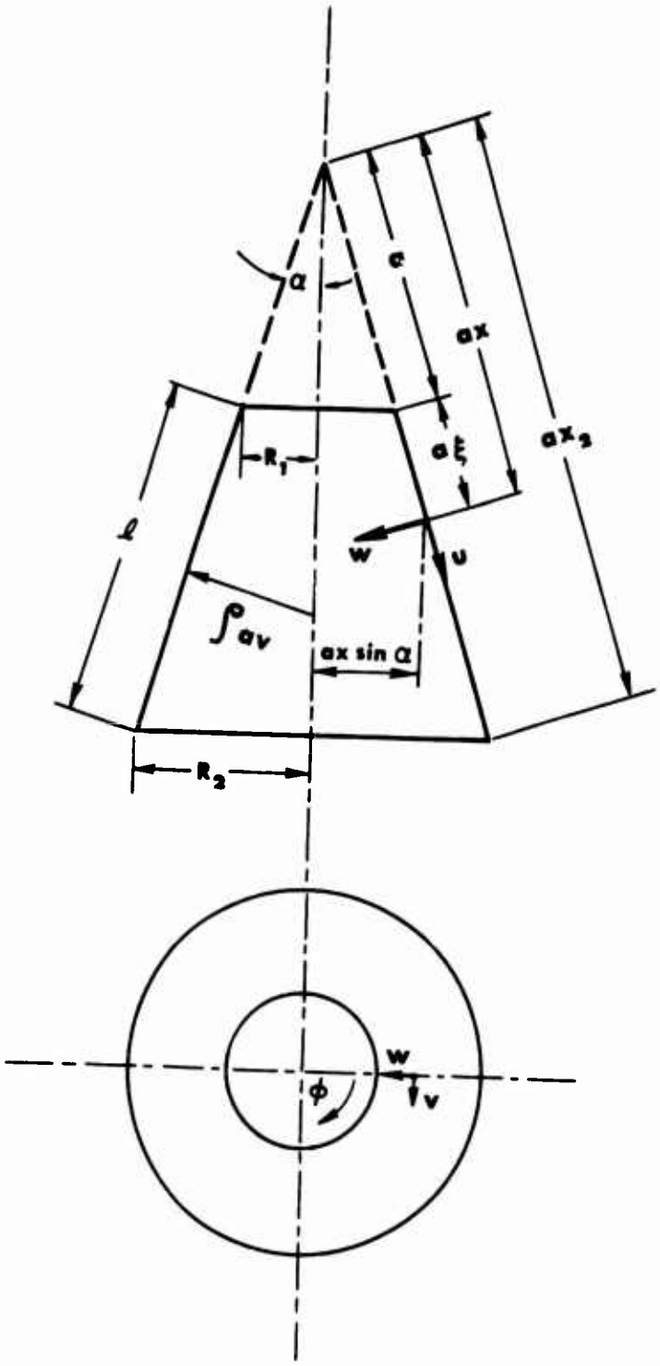

Figure 1. Notation.

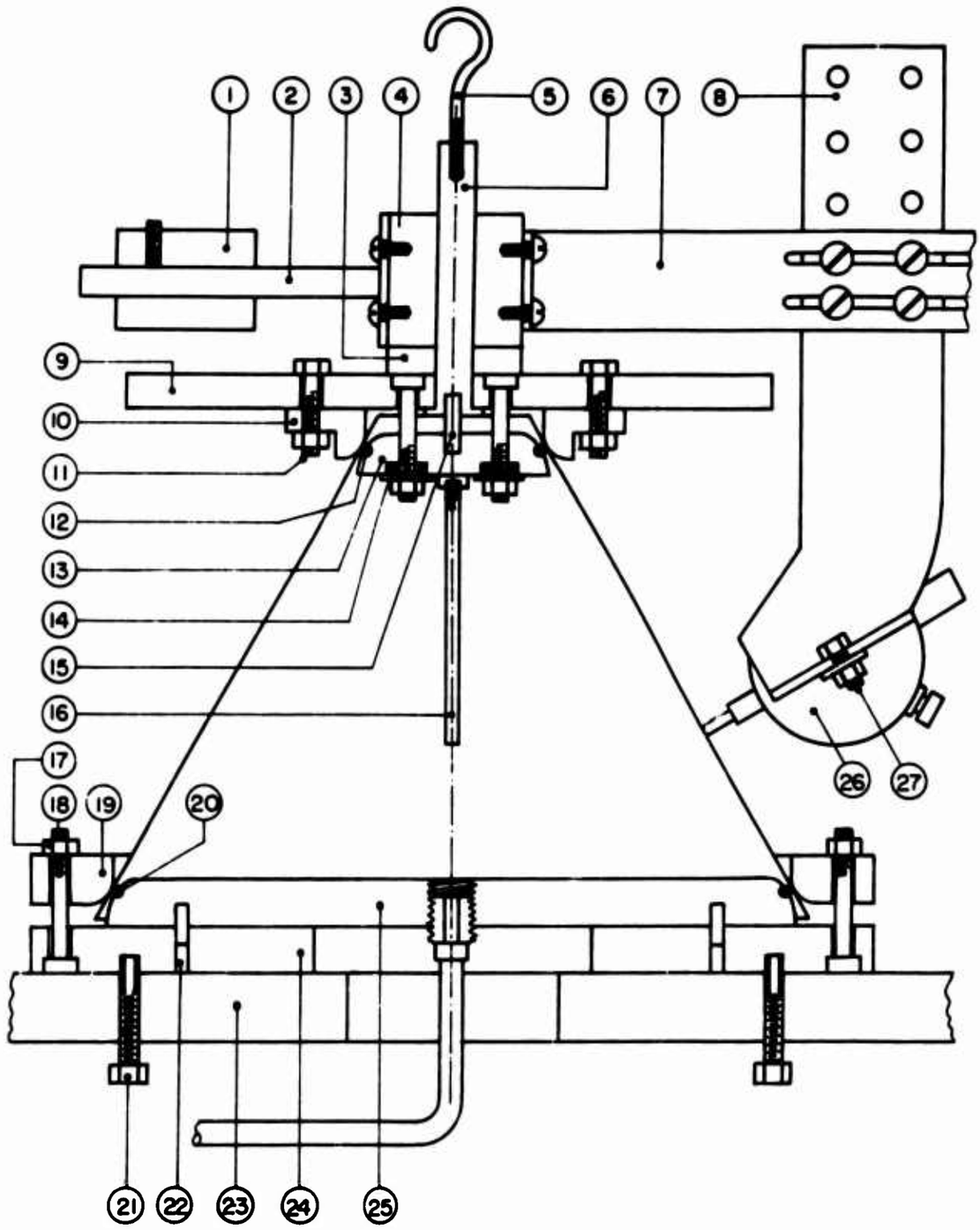

Figure 2. Specimen and Support Structure (Section View).

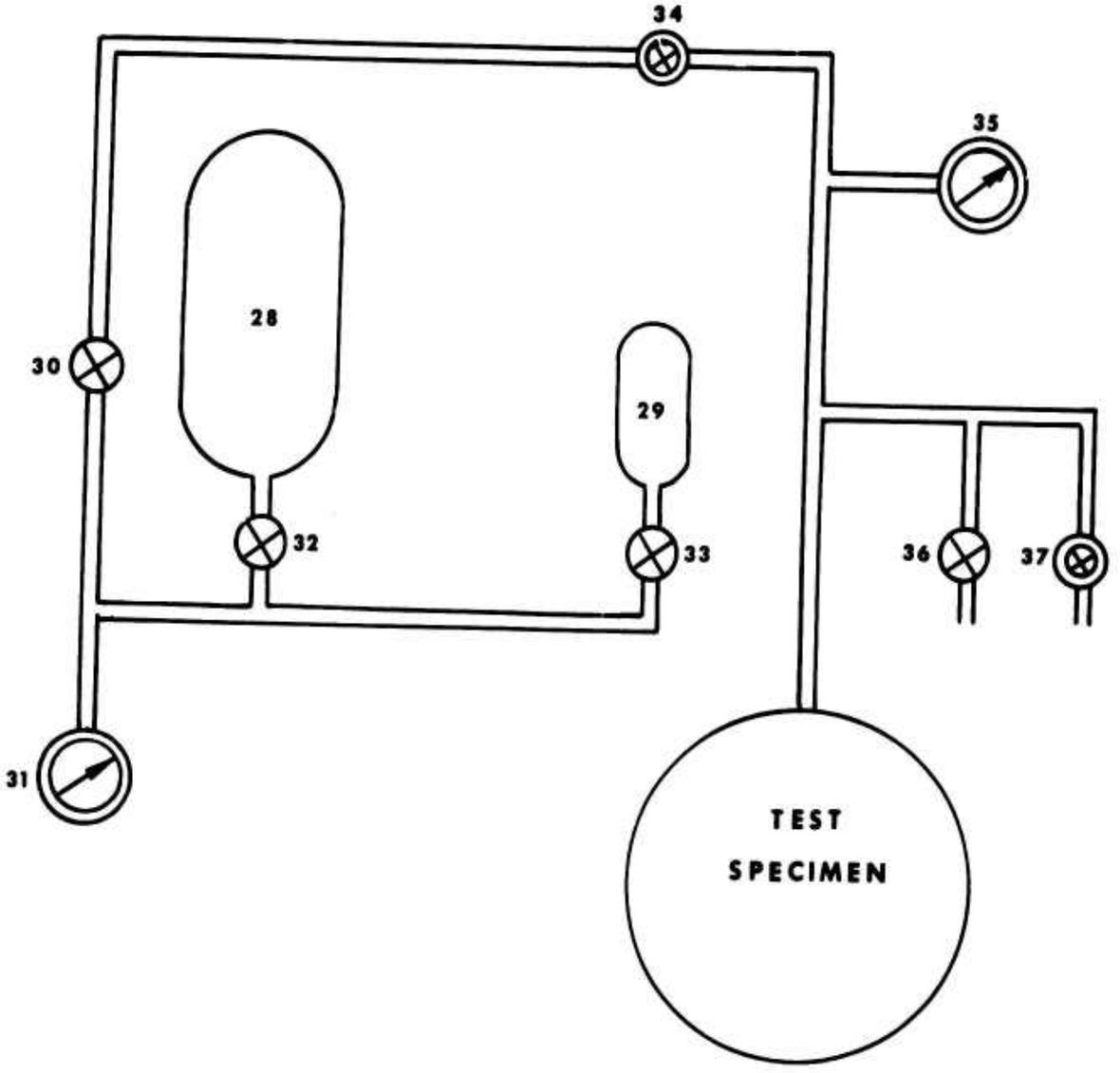

Figure 3. Vacuum and Pressure Measuring System.

hydrostatic pressure,[17,18] this effect is less sensitive to the length of the shell than clamping. Therefore, the boundary supports in the present experimental work represent an approximation to the theoretical simple support conditions of equation (1) similar to that of the Technion tests[1,2] and slightly better than that of the Space Technology tests.[3,4] The system was also found to be practically airtight.

The test rig consisted of the following components.*

THE SUPPORT FIXTURES

The system is set up on a rigid metal frame structure upon which a circular steel base disc is placed (24). This disc can be leveled to a true horizontal position by manipulation of three leveling screws(21). A steel base support disc(25) lies immediately atop the base disc. This disc is centered with respect to the rig axis by centering pins(22). The bottom O-seal(20) fits precisely into the support disc groove; it provides the only contact between the internal cone surface and the bottom support system. The external surface of the shell edge is supported by the base support ring(19), which, when bolted down(17) to the base disc, fixes the bottom support of the specimen. The support ring is also accurately centered with two centering pins which run through it to the base disc.

The top support structure is similar to the bottom one, except that its entire weight is supported, or counterbalanced, by a counterweight system (Figure 4) which is attached to a support hook(5). The hook is screwed into a support rod(6) upon which the top disc(9) rests concentrically. The rod itself acts as a centering pin to the disc. The top support ring(10) is bolted(11) to the top disc and centered with centering pins. Its rounded edges contact the upper external edge of the test specimen.

The shell is held in place by the top support disc(13) which is bolted to the top disc. The O-seal(12), embedded in the rounded edge of the support disc, provides the only contact between the internal surface of the shell and the top support system. The top support disc is centered with a centering pin(15) which extends from the support rod. Small O-seals(14) prevent air leakage into the specimen through the bolt holes.

THE OUT-OF-ROUNDNESS MEASURING DEVICE

The out-of-roundness measuring device consists of a steel block(4) which fits smoothly onto the support rod(6) and is centered by it. The block rests on a circular base disc(3). The upper surface of this disc and the bottom surface of the block have been given a very fine finish for easy movement of the block. A thin aluminum horizontal arm(7) is attached to one side of the block. It is provided with slots for horizontal adjustment of the vertical arm (8). Vertical adjustment is obtained by position-

*All numbers in superscript parentheses refer to part numbers in Figures 2,3,4,5 and 6. All major parts are listed on page 38 .

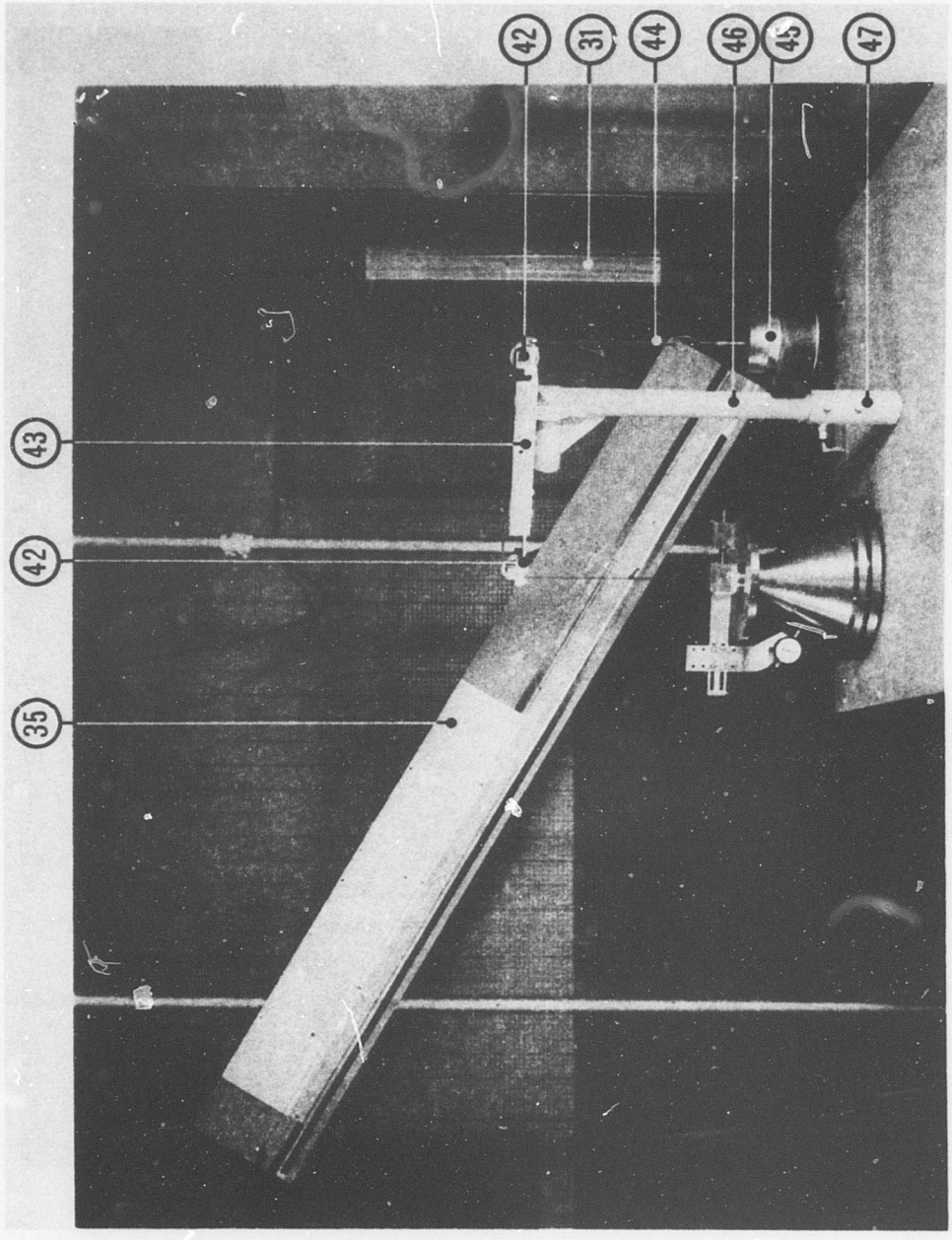

Figure 4. Test Rig With Manometer System.

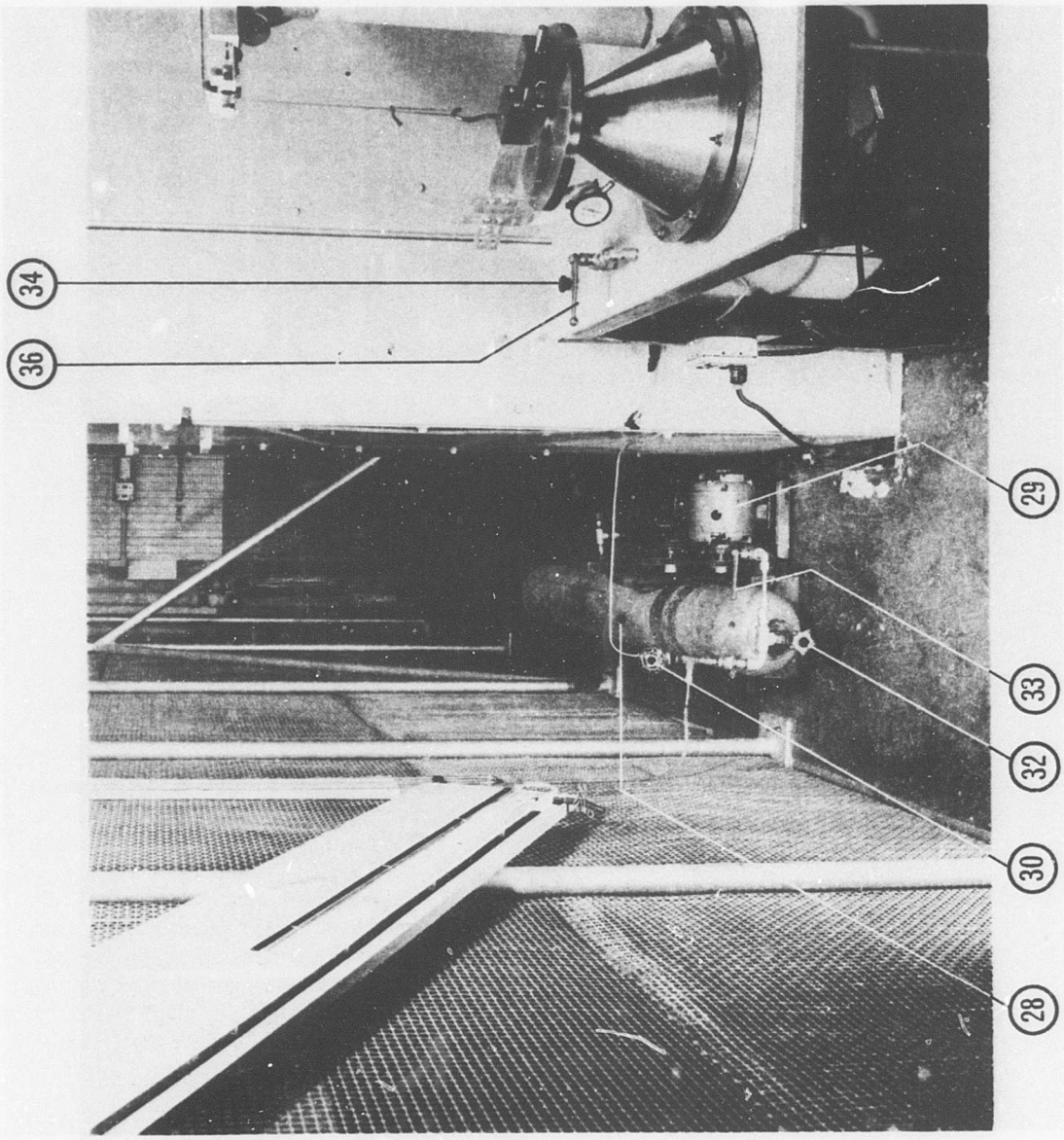

Figure 5. Test Rig and Vacuum System.

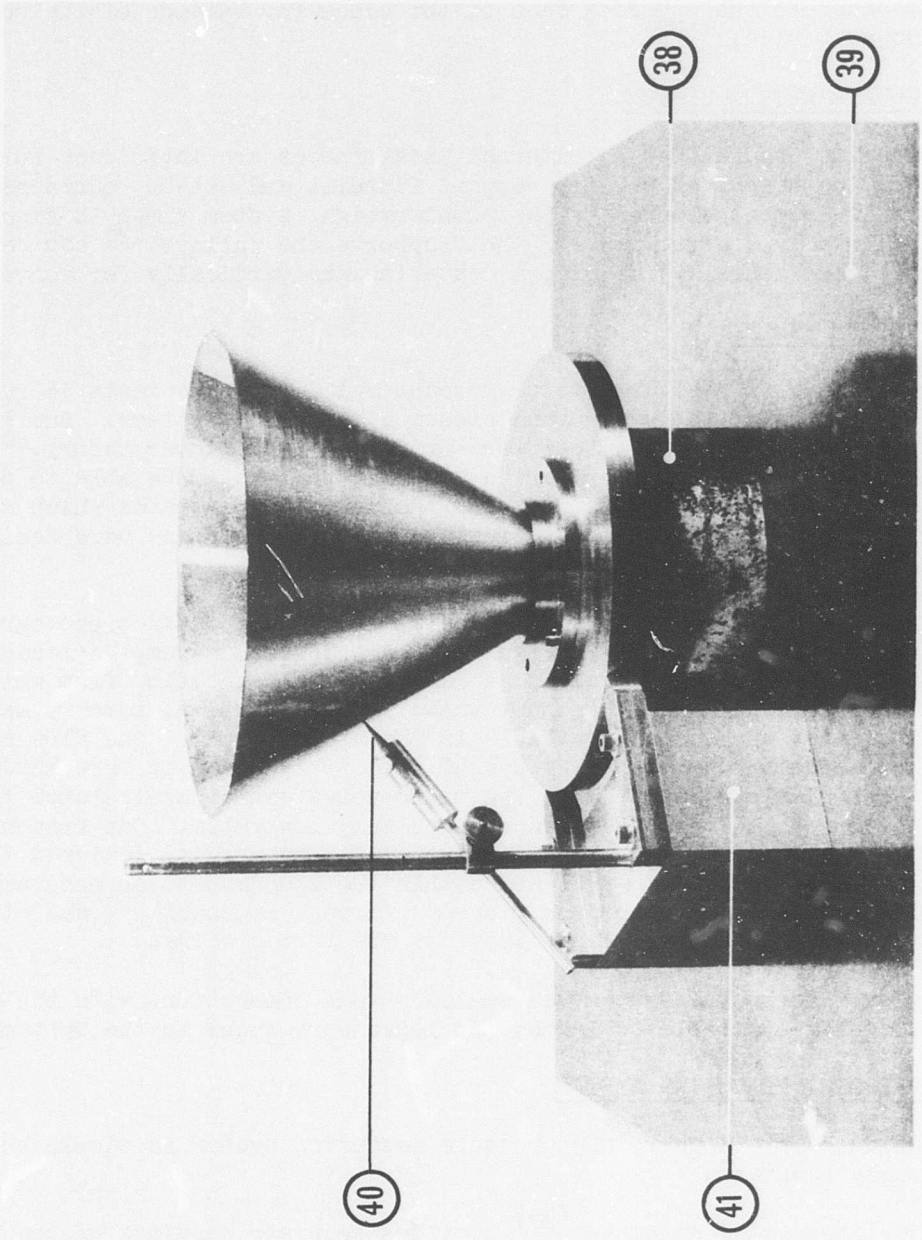

Figure 6. Shell Centering Device.

ing holes in the vertical arm. The dial gage(26) engages the shell specimen in a direction normal to the surface. Gage deflections could be read to an accuracy of ±.00005 inch.

A counterweight(1), which is free to slide along a horizontal shaft(2), is attached to the opposite face of the block for balance of the out-of-roundness device.

THE COUNTERWEIGHT SYSTEM

In order to ensure that no external axial forces are introduced into the system, the weight of the top support fixtures and out-of-roundness device is counterbalanced by the counterweight system shown in Figure 4. The gallows type structure(43) that supports the pulleys(42) can be adjusted horizontally for proper centering and vertically for convenience.

THE VACUUM SYSTEM

The magnitude of pressures to be encountered during the tests is required for the design of the vacuum and pressure measuring systems. Buckling pressures of .2 psi to 2.5 psi were predicted from linear theory.[10,11] Another important design criterion was that the system be able to provide smooth, nonoscillatory flow from the test specimen at rates which should approach zero. The vacuum and pressure measuring systems were designed with these criteria in mind.

The vacuum system is shown schematically in Figure 3, and a photograph of the system can be seen in Figure 5. A $\frac{1}{4}$ HP vacuum pump(29) leads through a valve(33) to a vacuum storage tank(28), the flow from which can later be regulated by another valve(32). A vertical mercury manometer (31) indicates the vacuum available in the storage tank. The flow line then proceeds through the main system valve(30), which in turn leads to the flow control micro-valve(34). The micro-valve can be manipulated to ensure evacuation of the test specimen at extremely low rates. One branch of the flow line then leads to an inclined water manometer(35), designed to indicate the decrease in pressure within the specimen to an accuracy of ±.0015 psi. The second branch proceeds through a manual(36) and electrical (37) solenoid pressure release valve to the test specimen.

The flow line of the system was sealed at all connections with the aid of commercially available sealants. No leaks were found in the system.

THE PRESSURE MEASURING SYSTEM

As mentioned previously, the pressure measuring system is simple but extremely accurate.

The inclined water manometer(35) provides accurate readings of the pressure in the test specimen throughout the test and in particular the pressure at buckling. The manometer was designed to cover the full range of expected buckling pressures, namely .2 psi to 2.5 psi. The manometer is over 8 feet

long and is inclined at an angle of 32^{o} 38' to the horizontal. Considering meniscus inaccuracies and the like, the accuracy with which the manometer could be read is approximately $\pm$2mm. Millimeter paper was inserted under the manometer tubes and calibrated values of pressure were marked off at equal intervals of .05 psi. Linear interpolation was used to obtain pressures between the marked intervals. Allowing for various inaccuracies, such as millimeter paper inaccuracies, interpolation errors, water density, etc., it would be safe to assume that the pressure readings are accurate to within $\pm$.004 psi, which within the working range of pressures produces a maximum error of less than 2 percent.

The accuracy of the vertical mercury manometer[31], which measures the pressure in the vacuum storage tank, is of no importance since it only indicates reservoir pressure.

TEST SPECIMENS

The specimens were very thin electroformed nickel shells of high uniformity. Details of their manufacture and thickness measurement are given in Appendix I, where the different techniques considered are also discussed.

Since the aim of the present tests was an investigation of the "hump" region, specimens of high taper ratio were required. Therefore, ten specimens of taper ratio 0.750 and three specimens of taper ratio 0.669 were made. The dimensions of the specimens are given in Table I, and a typical buckled specimen is shown in Figure 7. Only the average thickness is presented in Table I, since the thickness distribution was fairly uniform. In Table II this distribution is given for a typical shell W.122, and in Figure 12 the average thickness distribution along the generator of the shell is shown for all the specimens. In the circumferential direction, the thickness variation is very small in all the specimens (always less than 3 percent). In the axial direction, larger variations appear; but, as can be seen clearly in Figure 12, these variations are appreciable only at the ends of the shells - mostly within the end rings - where they have no effect. Even outside the end rings, thickness variations very near the ends have only negligible effect on the stiffness of the shell, unless rotation of generators is restrained.

If the variations near the ends are therefore omitted, the longitudinal thickness uniformity of the test shells is very high.

The specimens are of high radius-over-thickness ratio, the significant radius being the average radius of curvature of the cone

$$\rho_{av} = [(R_1 + R_2)/2 \cos \alpha] \qquad (3)$$

The shells tested cover a range of (ρ_{av}/h) roughly from 600 to 1300.

The out-of-roundness was measured for all but the thinnest specimens at a number of heights and did not exceed one-half of the thickness at any point. These measurements, together with the small scatter of thickness measurements, justify the classification of "good" for the shells tested.

To eliminate uncertainties, the Young's modulus of the electroformed nickel was determined from measurements on specimens taken from the actual shells. These very thin specimens posed a problem, since the attachment of strain gages for measurement of strain (the usual technique) could cause local stiffening and hence a significant error in E. An optical technique was tried but was found to be unsatisfactory because of excessive scatter. Finally, small BLH-type AF-7-1 gages (mounted on thin paper) were attached and the specimens were tested in an Instron Testing Machine. The values obtained from the strain gage readings were compared with those obtained from the direct displacement recording of the testing machine. By repeating the test after removal of strain gages, the stiffening effect of the strain gages could be estimated; an average 8 percent stiffening was found.

Except for the first three shells from which only one specimen each was tested, two specimens (or more) were cut from each of the shells, one along the generator and one in the circumferential direction. Many specimens were retested a number of times.

The mean value of $E = 28 \times 10^6$ psi was obtained without correction for the stiffening effect of the strain gages. This value coincides with that obtained for spherical shells manufactured in the same laboratories at the same time and by a similar technique.[19] In Reference 19 only five specimens were tested, and a relatively small scatter of $\pm 0.5 \times 10^6$ psi was noted. In the present tests, 24 specimens were tested and the scatter was larger: $+0.9 \times 10^6$ psi and -1.6×10^6 psi, if a few unreliable results (obtained by the optical technique and by direct recording only on the Instron) are excluded. No significant orthotropy was observed, and no trend of increase or decrease in E for early or later shells could be noticed. Hence, the average value $E = 28 \times 10^6$ psi is taken for all the shells. If the average stiffening effect of the strain gages is taken into account where appropriate, the Young's modulus reduces to $E = 26.5 \times 10^6$ psi.

Poisson's ratio was not measured, and the value obtained in Reference 19 for similarly electroformed nickel, $\nu = 0.10$, is assumed to be a low value; $\nu = 0.30$, the value usually quoted for nickel, is assumed to be a high value. The theoretical results are computed for both values of E and ν.

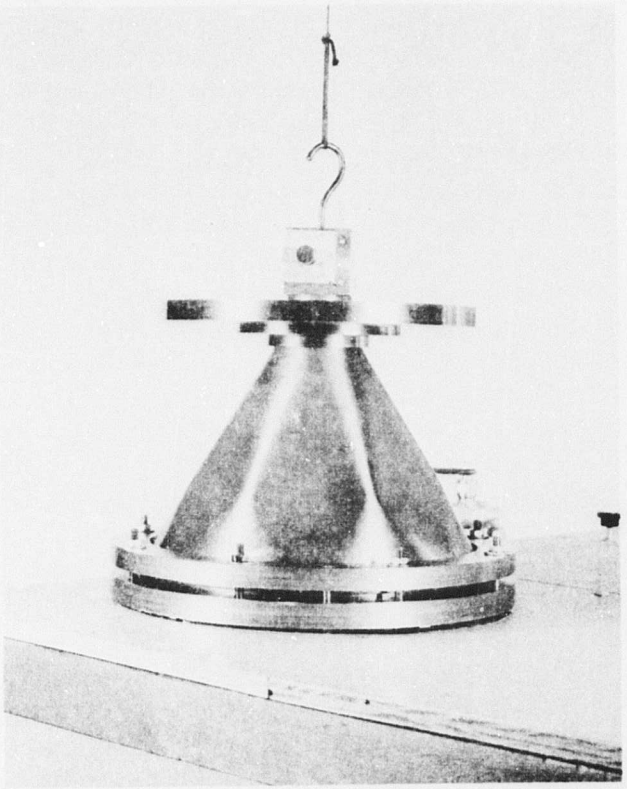

Figure 7. Fully Developed Elastic Buckling.

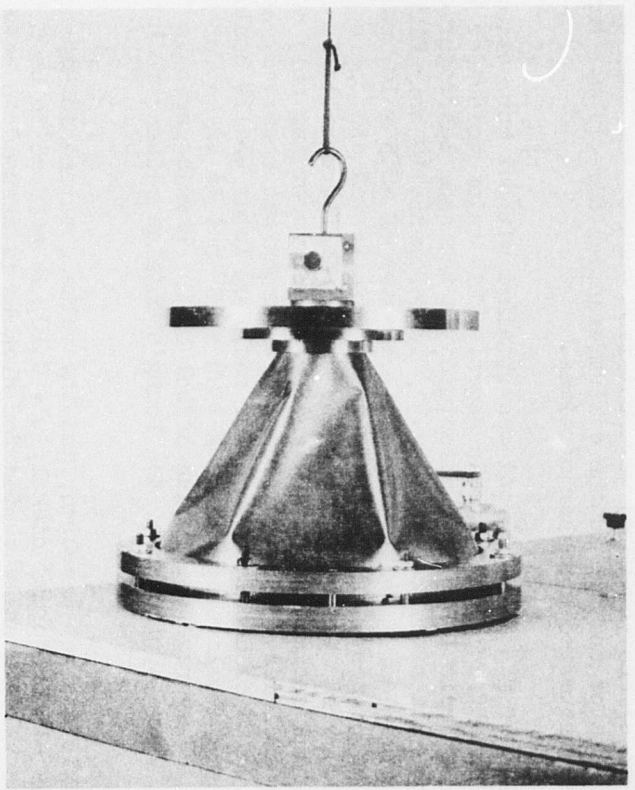

Figure 8. Onset of Plastic Buckling.

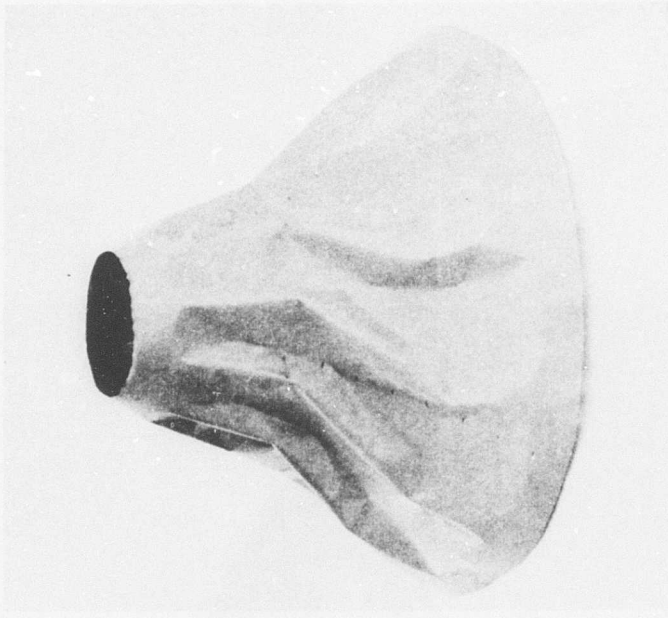

NOT REPRODUCIBLE

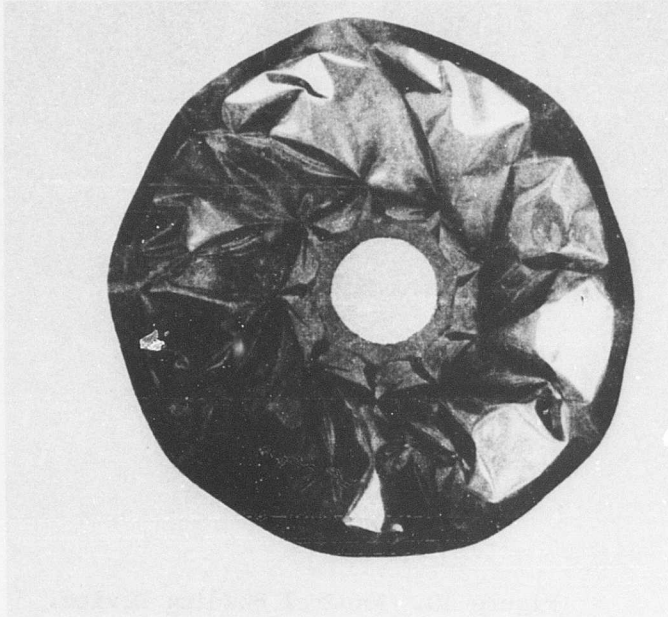

Figure 9. Plastic Collapse.

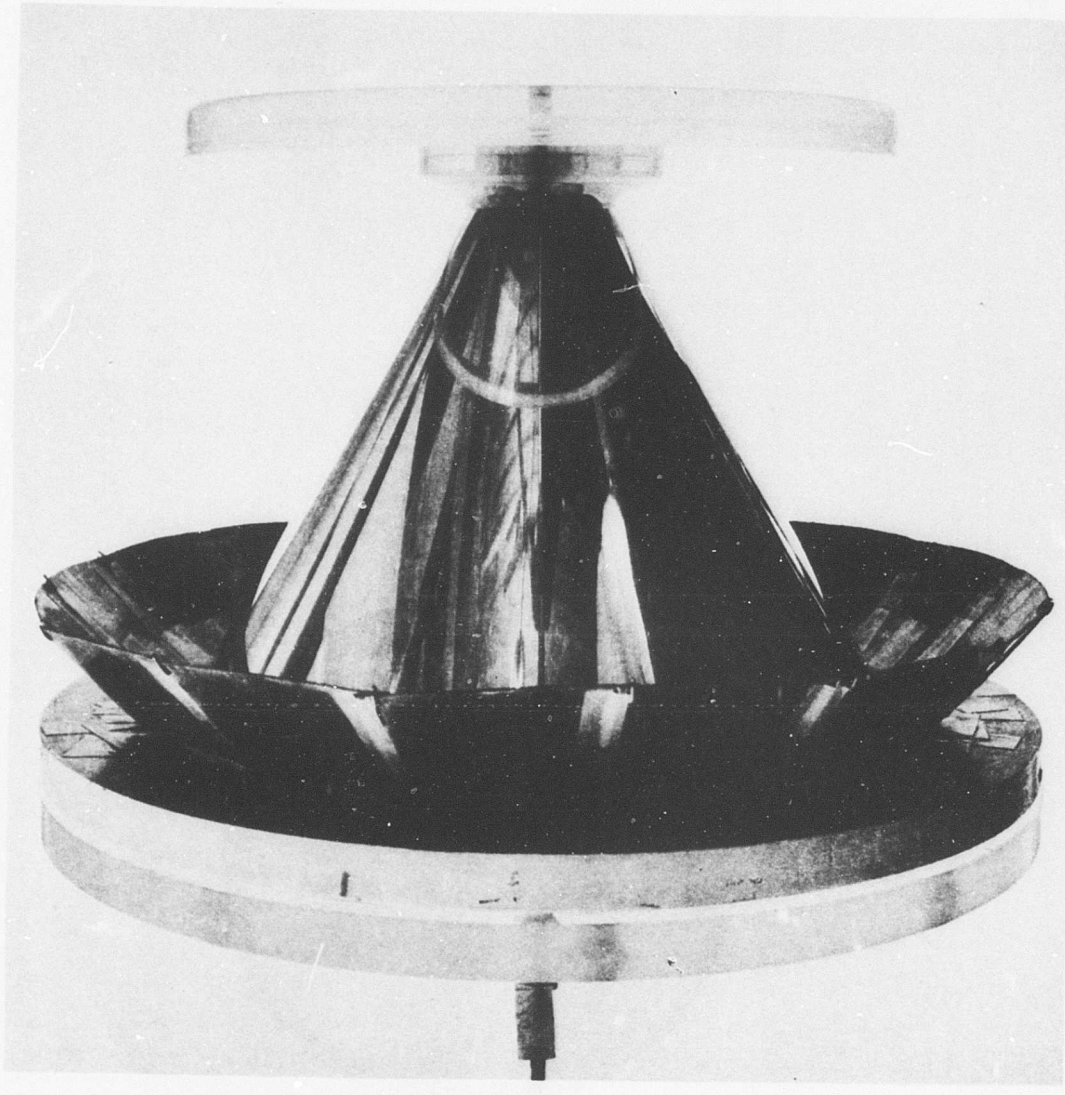

Figure 10. Mandrel Shading Device.

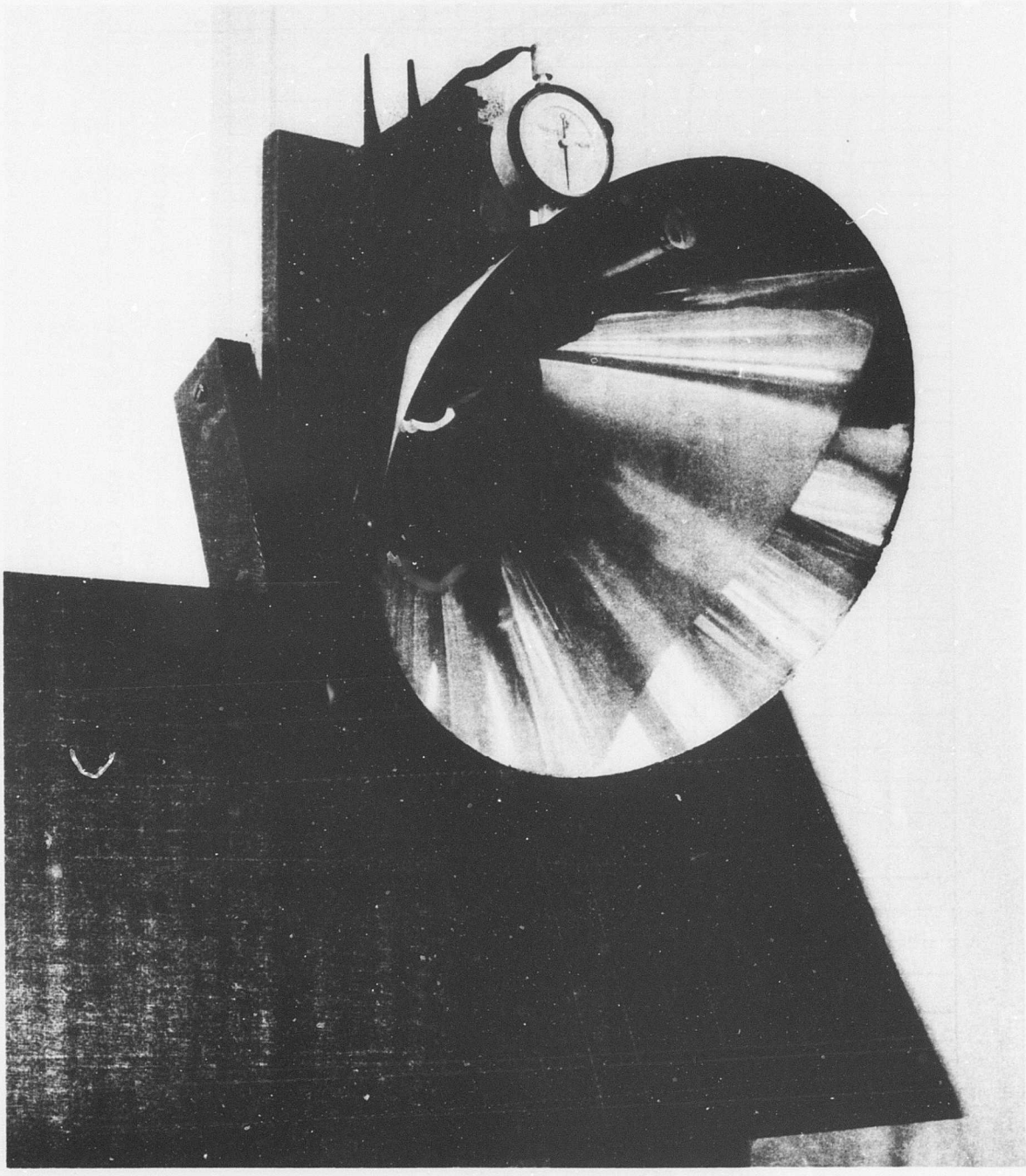

Figure 11. Thickness Measuring Apparatus.

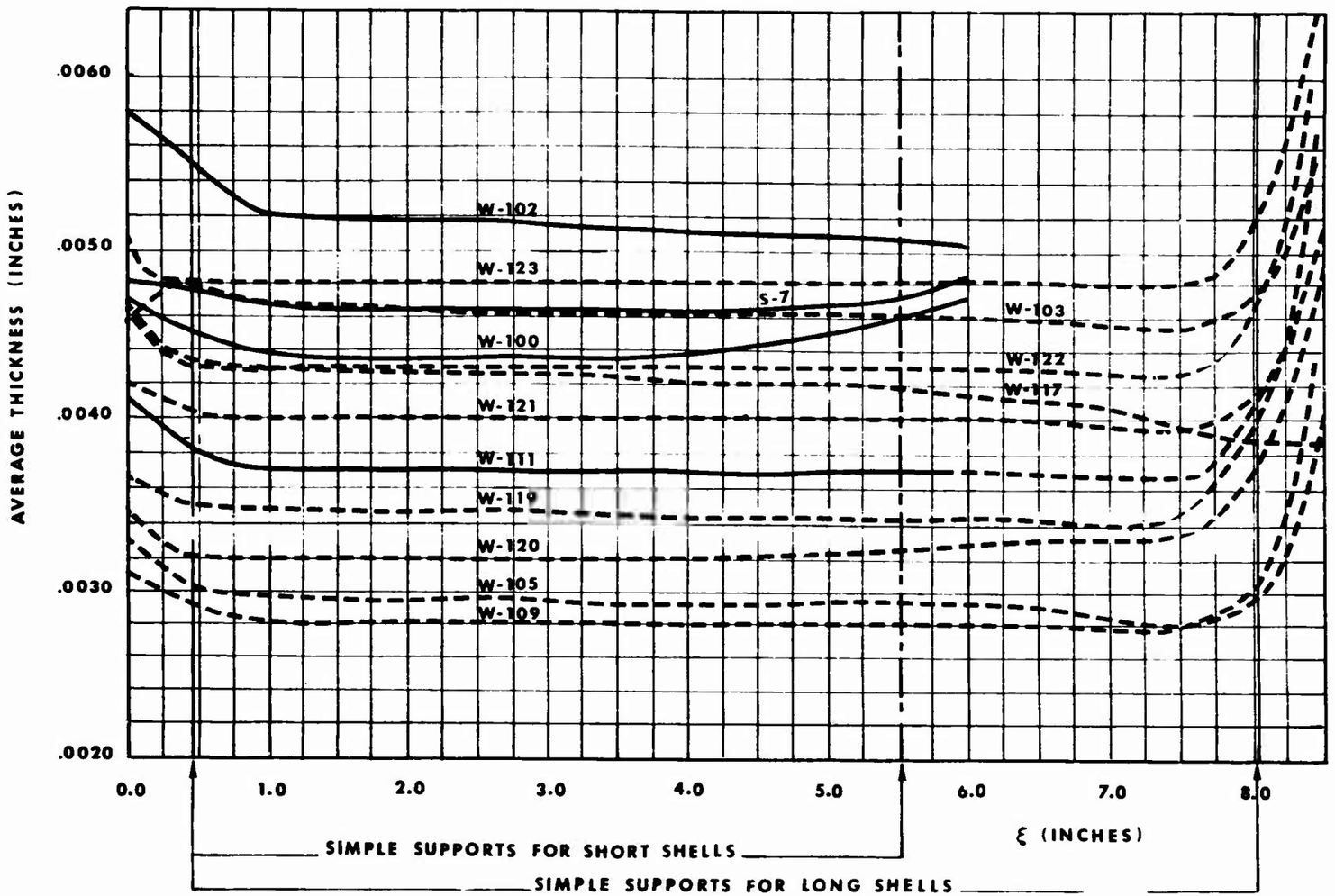

Figure 12. Average Thickness Distribution of Test Shells.

TABLE I. DIMENSIONS OF SPECIMENS

SPECIMEN	R_1 (INCHES)	R_2 (INCHES)	ψ TAPER RATIO	α	h_{av}	(ρ_{av}/h)
W·103	1.250	5.000	.750	30°	.00462	781
W·105	1.250	5.000	.750	30°	.00294	1227
W·109	1.250	5.000	.750	30°	.00281	1284
W·111	1.250	5.000	.750	30°	.00370	975
W·102	1.250	3.775	.669	30°	.00512	567
S·7	1.250	3.775	.669	30°	.00466	623
W·100	1.250	3.775	.669	30°	.00444	653
W·117	1.250	5.000	.750	30°	.00420	859
W·119	1.250	5.000	.750	30°	.00344	1049
W·120	1.250	5.000	.750	30°	.00324	1114
W·121	1.250	5.000	.750	30°	.00400	902
W·122	1.250	5.000	.750	30°	.00430	839
W·123	1.250	5.000	.750	30°	.00481	750

TABLE II. THICKNESS DISTRIBUTION FOR SPECIMEN W·122

ξ.in. \ φ°	0°	90°	180°	270°	AVERAGE
0	.00470	.00455	.00470	.00465	.00465
.5	.00430	.00432	.00430	.00431	.00431
1.0	.00430	.00430	.00430	.00431	.00430
1.5	.00430	.00430	.00430	.00431	.00430
2.0	.00430	.00430	.00430	.00431	.00430
2.5	.00430	.00430	.00430	.00431	.00430
3.0	.00430	.00430	.00430	.00431	.00430
3.5	.00430	.00430	.00430	.00431	.00430
4.0	.00430	.00430	.00430	.00431	.00430
4.5	.00430	.00430	.00429	.00431	.00430
5.0	.00430	.00430	.00429	.00431	.00430
5.5	.00430	.00430	.00429	.00431	.00430
6.0	.00430	.00430	.00429	.00431	.00430
6.5	.00430	.00430	.00427	.00431	.00429
7.0	.00430	.00428	.00425	.00431	.00428
7.5	.00432	.00420	.00423	.00431	.00426
8.0	.00490	.00433	.00450	.00481	.00463
8.5	.00750	.00585	.00650	.00680	.00665

TEST PROCEDURE AND TECHNIQUE

ASSEMBLY TECHNIQUE

The assembly procedure carried out routinely is as follows. The base disc(24) is set down upon the base plate(23), and the level adjusting screws(21) are inserted into their respectively positioned holes. The base disc is then leveled to true horizontal with the aid of an accurate builder's level. The countersunk bolts(18) which have previously been inserted into their slots are now restricted from rotating. The base support disc(25), with its O-seal(20), is then centered upon the base disc(24) by the centering pins(22).

Now the top support rod(6) is inserted through the center hole of the top disc(9), and the top support ring(10) is concentrically placed below the top disc, centering being again achieved by prematched centering pins through the support ring and top disc. The bolts(11) are than tightened, and the other bolts are inserted into the top disc and taped down.

The partial top assembly is then inverted and put upside down upon a long hollow ring(38) as shown in Figure 6. Thus, the top disc face rests upon the ring while the support rod(6) hangs suspended through the ring. The test specimen is then placed, with its small radius down, upon the rounded edges of the top support ring(10), as shown in Figure 6. The inverted system is then leveled on a true level plate(39).

The top support disc(13) with its O-seal(12) is then gently lowered with the aid of a detachable rod(16) into the inverted shell until the centering pin(15) engages its mated hole. Small O-seals(14) are then slipped over the protruding bolts, followed by washers and nuts.

A centering device, shown in Figure 6, is then used for positioning the shell within the supports. The pencil-point indicator(40) is adjusted normal to the shell surface, and the device(41) is slid freely about the shell assembly. The cone position is continuously adjusted until the distance between the pencil point and the shell surface remains unchanged. The nuts are then manually tightened until a certain minimum resistance is encountered. On one hand, it is desirable to tighten these nuts as much as possible in order to ensure proper sealing. On the other hand, however, when tight bolts are maintained, the O-seals tend to flatten out and the simulation of the boundary condition permitting edge rotation is impaired. Also, excessive tightening of the nuts produces ripples in the shell skin which cause premature buckling.

It was found that excellent sealing is maintained even when the nuts are barely tightened. A sensitive torque wrench was used to ensure equal tightening of the nuts.

The next step in the assembly is unscrewing the detachable rod(16) and removing the cone assembly from the centering device. The out-of-roundness device base ring(3) and block(4) are then slipped into position onto the top support rod(6), and the counterweight hook(5) is also screwed

into position. The base support ring(19) is then slipped over the fixture and held level with the top disc(9) as the entire assembly is hooked onto the nylon counterweight string(44). Weights(45) are added until the system is in equilibrium.

The 'dangling' system is then slowly allowed to descend until the bottom edge of the cone rests lightly upon the bottom O-seal(20). The base support ring(19), which was previously held level with the top disc, is finally let down, centered with prematched centering pins, and allowed to come to rest upon the outer surface of the cone. The nuts(17) are then tightened in the same manner as the top nuts.

The vertical(8) and horizontal(7) arms of the out-of-roundness device are next adjusted and fixed such that the deflection dial gage(26) is slightly preloaded on the surface of the shell. The device is then rotated 360°, and deflection measurements are taken at various intervals. (This method was used only for the thicker specimens where the gage spring did not cause local buckling of the shell surface.) The setup is now ready for testing.

VACUUM SYSTEM TECHNIQUE

All valves are initially closed except (32) and (33) of Figure 3. The vacuum pump(29) is then operated until the pressure in the tank(28) falls to a value of approximately 8 psi. The vacuum pump is then shut off, and the valve(33) is closed to prevent leakage through the pump. The vacuum supply in the tank is now sufficient to last for the duration of many tests, and it is not necessary to operate the pump.

The main system valve(30) is then partially opened and the actual evacuation of the shell is begun by slowly opening the micro-valve(34). The micro-valve completely controls the rate of evacuation from the shell. Throughout the test, this rate is kept down to approximately .005 psi/sec, so that the precise buckling pressure reading could be visually located on the manometer at the instant of buckling. As the pressure in the shell slowly falls, the observer stands by the manometer and holds the push-button pressure release solenoid valve in one hand; in the other hand he holds a thin wire indicator with which he follows the water level in the manometer. At the precise moment of buckling, an immediate pressure rise and a 'pop' sound occur. The observer immediately releases the vacuum by depressing the solenoid valve button and thereby allows an immediate snap-back of the shell to its original shape. The buckling pressure is then recorded and the system is ready for the next test.

In the present study, each specimen was buckled at least four times in succession. The successive buckling pressures for all specimens exhibited a general trend of the type shown in Figure 13. The first pressure is the actual buckling pressure, whereas the others are lower due to minute plastic deformations encountered during previous buckles.

When each specimen was buckled for the final time, the pressure was not

released and the fully buckled shape was studied (Figure 7). In some cases the specimens were then further evacuated to permit study of the plastic buckling pattern (Figure 8). These latter shells were also brought to the state of actual plastic collapse as depicted in Figure 9.

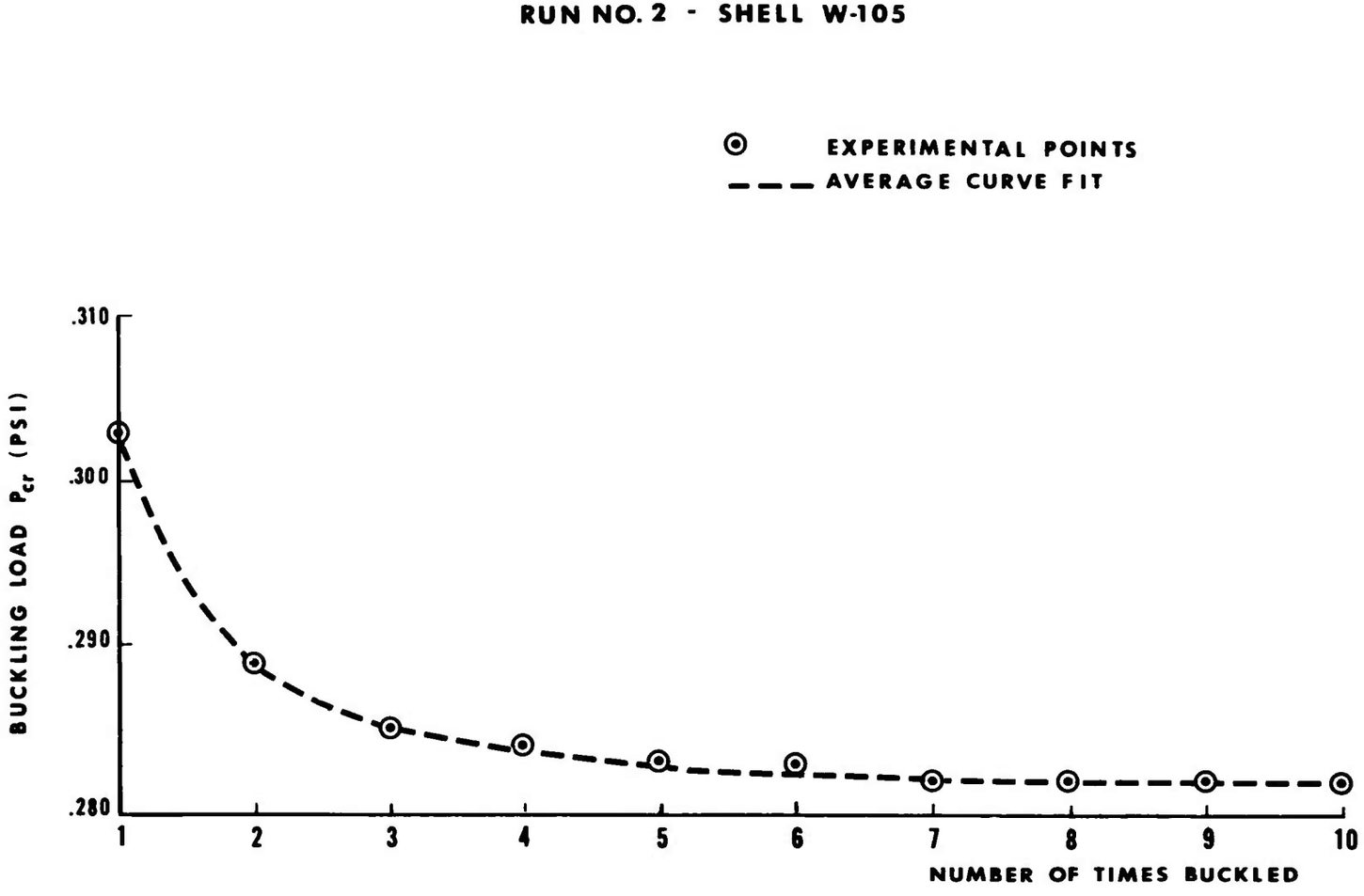

Figure 13. Buckling Load vs. Number of Times Shell Buckled.

EXPERIMENTAL RESULTS AND CORRELATION WITH THEORY

The buckling pressures obtained for the 13 shells are presented in Table III. The value recorded is the pressure at which the shell buckled for the first time, as observed visually on the inclined manometer. The simple technique described in the previous section proved to be of satisfactory accuracy. Due to the high quality of the shells, buckles appeared around the whole circumference simultaneously in all of the specimens. Hence, no differentiation between onset of buckling and complete buckling, as used in References 1 and 2, was required. Here, as for the better specimens of Reference 2, onset of buckling and complete buckling occurred simultaneously.

All the shells were buckled a number of times, and the repeated buckling (see Figure 13) showed a similar reduction of buckling load, with a trend to an asymptotic value, as observed in Reference 20 for cylindrical and conical shells under axial compression. Here, for buckling under hydrostatic pressure, however, the reduction in load due to repeated buckling is much smaller; for example, 7% in Figure 13 as compared to about 30% for the conical shell under axial compression in Reference 20. This difference is mainly due to smaller imperfection sensitivity of shells buckling under hydrostatic pressure.

The correlation with linear theory is summarized in Table III. The theoretical pressures $\bar{p}$ are the critical pressures for equivalent cylindrical shells, defined in References 14, 10 and 2 as the cylinder for which

$$\begin{aligned} R &= \rho_{av} \\ L &= \ell \\ h &= h \end{aligned} \tag{4}$$

The average radius of curvature ρ_{av} was defined by equation (3). The critical pressure of the equivalent cylindrical shell is computed with an approximate formula,[9,10] which because of equation (4) becomes

$$\bar{p} = \left[\frac{\pi/6}{9(1-\nu^2)}\right] E \left(\frac{h}{\rho_{av}}\right)^{2.5} \left(\frac{\rho_{av}}{\ell}\right) \tag{5}$$

The approximation implied by equation (5) for cylindrical shells consists of the smoothing out of the ripples in the resulting curves caused by the finite number of circumferential waves into which a shell buckles, and it is certainly justified here for t = 7,8,9. It should be pointed out that the numerical factor in square brackets in equation (5) is usually quoted as 0.918, its value when $\nu = 0.1$ (Reference 19) differs considerably from 0.3, the high value, the appropriate value of the factor 0.862 is used for $\nu = 0.1$.

The correlation between conical shells and equivalent cylindrical shells is expressed by a correlation function g that is primarily a function of

TABLE III. TEST RESULTS: EXPERIMENT VS. THEORY (FOR CLASSICAL SIMPLE SUPPORTS)

TEST NO.	SPECIMEN	ψ	TEST P_{cr} (PSI)	t	CORRELATION $E = 28 \times 10^6$ PSI, $\nu = .1$ $\bar{p}$(PSI)	$E = 28 \times 10^6$ PSI, $\nu = .1$ $g(\psi)$	$E = 28 \times 10^6$ PSI, $\nu = .3$ $\bar{p}$(PSI)	$E = 28 \times 10^6$ PSI, $\nu = .3$ $g(\psi)$	$E = 26.5 \times 10^6$ PSI, $\nu = .1$ $\bar{p}$(PSI)	$E = 26.5 \times 10^6$ PSI, $\nu = .1$ $g(\psi)$	$E = 26.5 \times 10^6$ PSI, $\nu = .3$ $\bar{p}$(PSI)	$E = 26.5 \times 10^6$ PSI, $\nu = .3$ $g(\psi)$	$g(\psi)$ REF. 12
1	W·103	.750	.854	8	.681	1.25	.725	1.18	.644	1.33	.686	1.24	1.22
2	W·105	.750	.303	9	.220	1.38	.234	1.29	.208	1.46	.222	1.37	1.22
3	W·109	.750	.268		.196	1.37	.209	1.28	.186	1.44	.198	1.35	1.22
4	W·111	.750	.519	8	.391	1.33	.416	1.25	.370	1.40	.394	1.32	1.22
5	W·102	.669	2.19	7	1.813	1.21	1.931	1.13	1.716	1.28	1.828	1.20	1.18
6	S·7	.669	1.88	8	1.433	1.31	1.526	1.23	1.356	1.39	1.445	1.30	1.18
7	W·100	.669	1.76	9	1.270	1.39	1.353	1.30	1.202	1.47	1.280	1.38	1.18
8	W·117	.750	.750	9	.536	1.35	.571	1.27	.508	1.43	.541	1.34	1.22
9	W·119	.750	.453	8	.326	1.39	.347	1.31	.308	1.47	.328	1.38	1.22
10	W·120	.750	.402	9	.280	1.43	.299	1.35	.265	1.52	.283	1.42	1.22
11	W·121	.750	.628	8	.475	1.32	.506	1.24	.449	1.40	.479	1.31	1.22
12	W·122	.750	.768	7	.569	1.35	.606	1.27	.538	1.43	.574	1.34	1.22
13	W·123	.750	.971		.753	1.29	.802	1.21	.713	1.36	.759	1.28	1.22

the taper ratio,[10,11]

$$(p/\bar{p}) = g(\psi), \tag{6}$$

though for large cone angles it depends also on the cone angle.[12] The values of g computed from the experimental buckling pressures and theory are given in Table III. The critical pressures of the equivalent cylinders are given for the two values of E, as discussed on page 12 : for $E = 28 \times 10^6$ psi, when the stiffening of the strain gages has not been accounted for, as well as for the two values of ν. In Figure 14, the values of $g(\psi)$ computed from the experimental results are superimposed on a theoretical correlation curve.[11,12] Figure 14 shows clearly that the doubts expressed in Reference 4 about the validity of the linear theories of References 10 and 11 in the "hump" region are unfounded. The conclusions of References 1 and 2 are therefore reconfirmed.

It is of interest to compare the experimental results with a recent analysis that takes the in-plane boundary conditions into account.[18] In Table IV such a comparison is presented for one shell, W.121. The theory of Reference 18 assumes simple supports for the radial displacement w ($w = M_x = 0$). As discussed on page 2 , the test apparatus approximates the conditions on w fairly well. However, there is a considerable amount of axial constraint in the test setup, and the test conditions are therefore between SS3 and SS4. The circumferential constraint is not important for hydrostatic pressure loading, but the test conditions are probably nearer to $v = 0$ than to $N_x = 0$. Table IV (in which, for clarity, the theoretical results are given only for $E = 28 \times 10^6$ psi and $\nu = 0.1$) explains why the test results fall above the theoretical correlation curve in Figure 14. The test result, $p_{cr} = 0.628$ psi, is 8% above the theoretical critical pressure for a conical shell on classical simple supports (SS3), whereas it is 23.5% below that for complete axial restraint (SS4). Since the test conditions are between SS3 and SS4, this result is a few percent below the theoretical predictions for a perfect shell, as one could expect for a good specimen. However, when correlated with an equivalent cylindrical shell on classical simple supports, as in Figure 14, it yields a point considerably above the theoretical curve of Reference 12, due to the stiffer boundary conditions of the test. To emphasize this argument, one could consider, for example, the value of $(p_1/\bar{p}) = 1.73$ for SS4 in Table IV, which indicates how far above the curve of Reference 12 a point for a perfect specimen with complete axial restraint would fall. It should therefore always be borne in mind that the classical simple supports are a conservative simulation of actual conditions that include axial constraint. This is one reason for the good agreement with predictions from "simple support" theory usually obtained by experiments for cylindrical and conical shells under external pressure, as already pointed out in Reference 18.

Since the effect of axial constraint is of similar magnitude for cylindrical shells, the conclusions about the validity of the correlation curve are not influenced by the in-plane boundary condition effects shown in Table IV. Correlation between conical shells with SS4 boundary conditions and equivalent cylindrical shells with SS4 conditions would yield a curve with a "hump" similar to that obtained for SS3 supports.

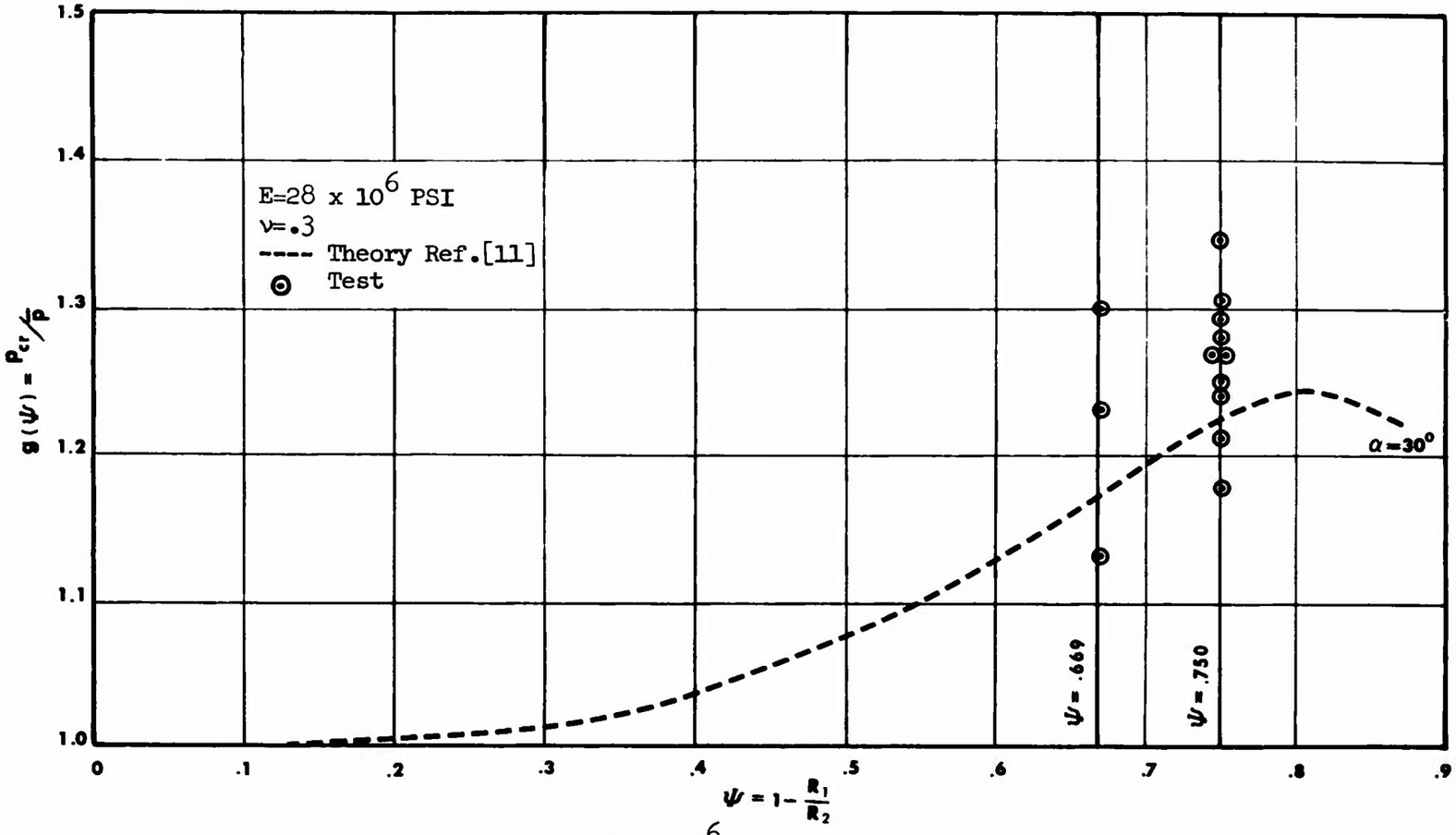

a. $E = 28 \times 10^6$ psi, $\nu = .3$.

Figure 14. Test Results ($P_{cr}\sqrt{\bar{p}}$ vs. ψ).

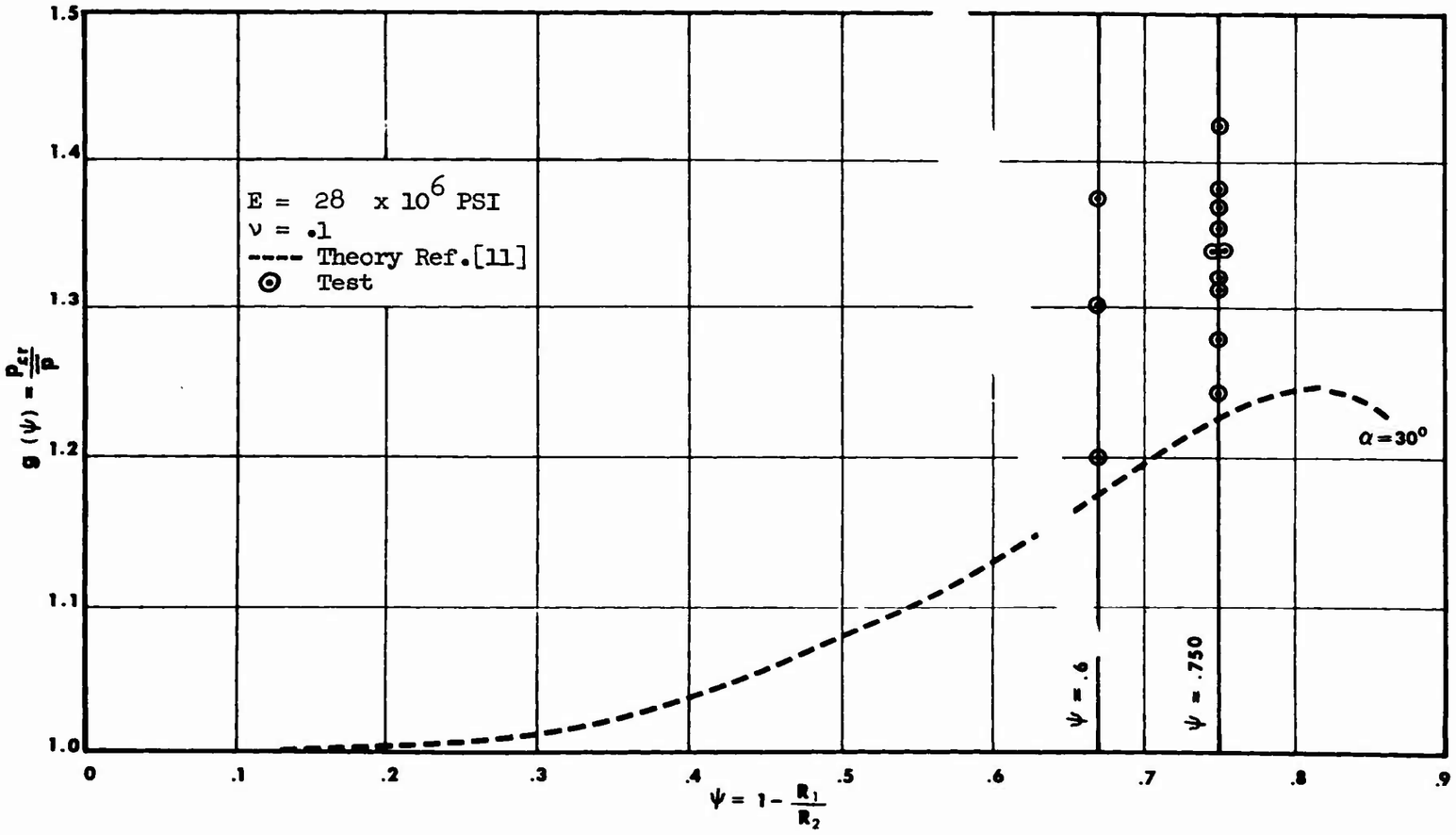

b. E = 28 x 10^6 psi, ν = .1.

Figure 14. Continued.

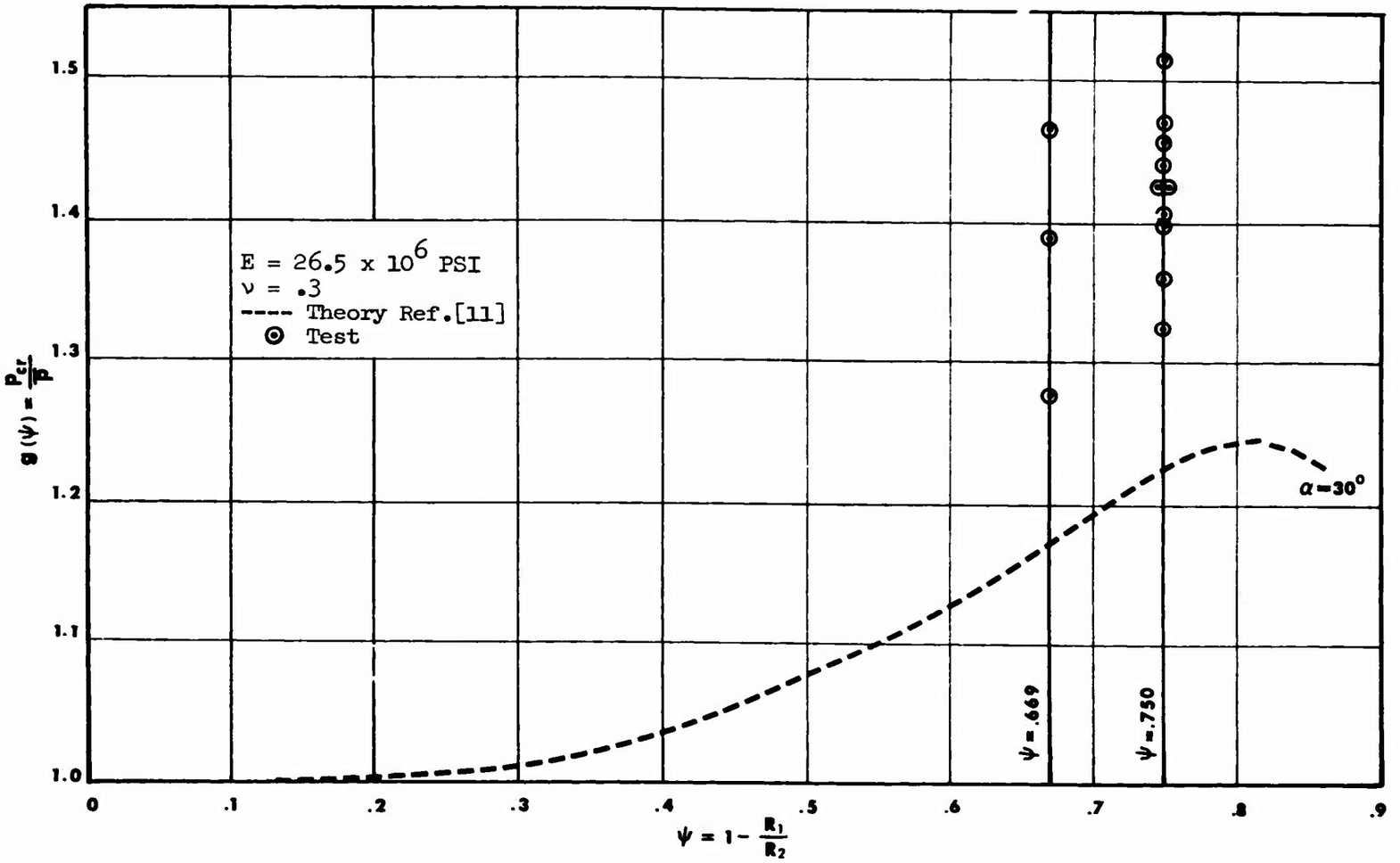

c. E = 26.5 x 10^6 psi, ν = .3.

Figure 14. Continued.

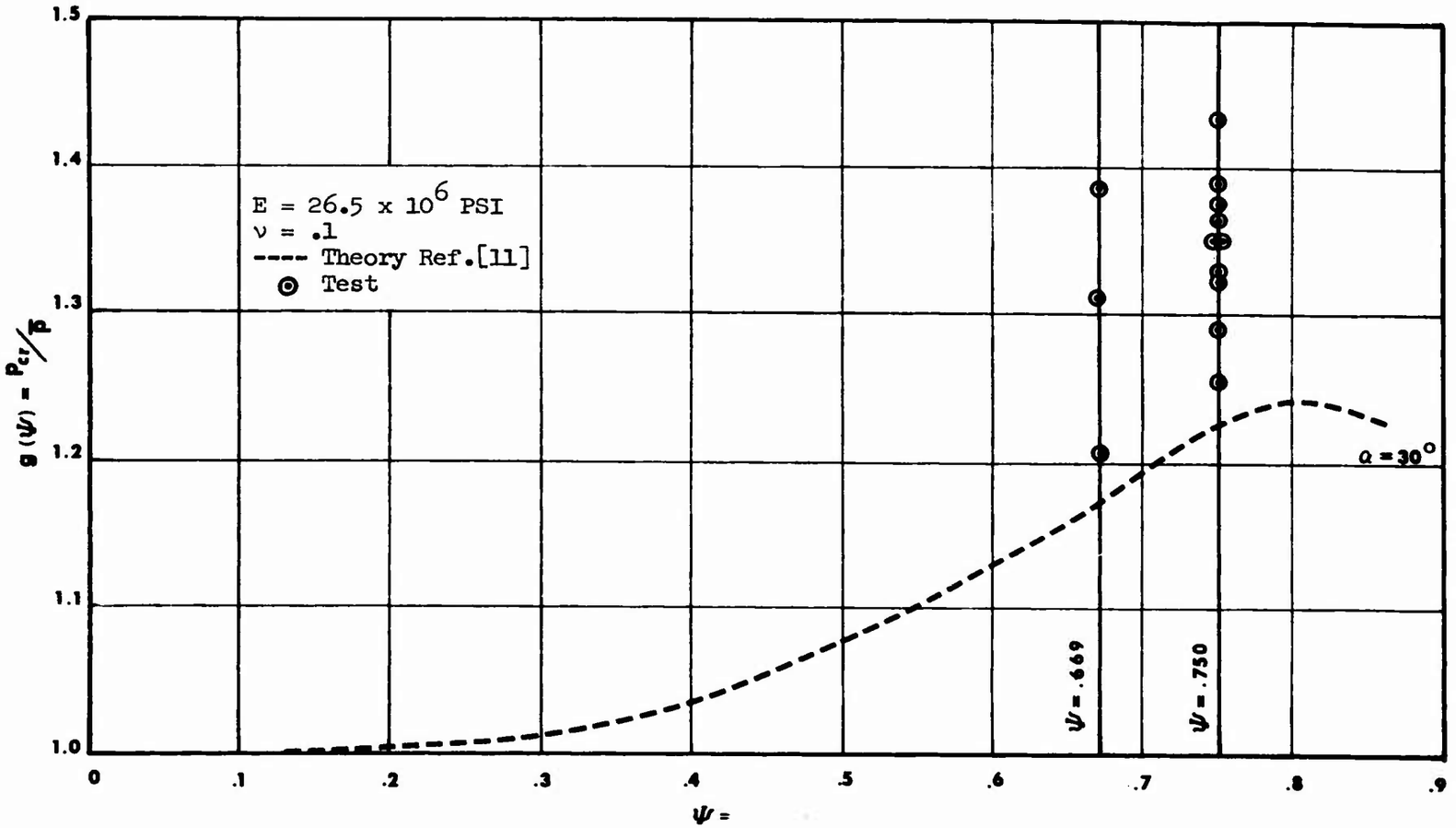

d. E = 26.5 x 10^6 psi, ν = .1.

Figure 14. Continued.

TABLE IV. CORRELATION WITH THEORY FOR DIFFERENT IN-PLANE BOUNDARY CONDITIONS (SPECIMEN W.121)

SHELL NO. W.121				$E = 28 \times 10^6$ PSI		
$w = M_x = 0$				$\nu = .1$		
IN-PLANE BOUNDARY CONDITIONS		CLASSICAL	SS1	$N_{x\varphi} = N_x = 0$		
			SS2	$N_{x\varphi} = u = 0$		
			SS3	$v = N_x = 0$		
			SS4	$v = u = 0$		
IN-PLANE BOUNDARY CONDITION	TEST p_{cr} (PSI)	p_1 THEORY CONICAL SHELL (REF. 18) (PSI)	$\frac{p_{cr}}{p_1}$	CORRELATION WITH EQUIVALENT CYLINDRICAL SHELL ON "CLASSICAL" BOUNDARY CONDITIONS		
				FROM REF. 12 $\frac{p_{th}}{\bar{p}}$	$\frac{p_1}{\bar{p}}$	$\frac{p_{cr}}{\bar{p}}$
SS 1	.628	.575	1.09	1.22	1.21	1.32
SS 2		.807	.778		1.70	
SS 3		.582	1.08		1.22	
SS 4		.821	.765		1.73	

CONCLUSIONS

By careful development of an electroforming process, very thin nickel conical shells of high uniformity were produced. The good quality of the specimens resulted in buckling pressures that were slightly above those predicted by linear theory for classical simple supports. The simplicity of the test rig, the vacuum system, and the pressure measuring system facilitated testing, and careful assembly and testing permitted repeated buckling with small reductions in buckling load. A trend to an asymptotic value of buckling load about 10% below the initial value was observed after repeated buckling.

Correlation with linear theories of Seide and Singer also confirms the validity of these theories for large taper ratios in the "hump" region of the correlation curve. The effect of axial constraint, not taken into account in these earlier theories but considered recently, explains the relatively high experimental buckling pressures obtained.

REFERENCES

1. Singer, J., and Eckstein, A., EXPERIMENTAL INVESTIGATION OF THE INSTABILITY OF CONICAL SHELLS UNDER EXTERNAL PRESSURE, Proceedings of the Fourth Annual Conference on Aviation and Astronautics, February 1962, Bulletin of the Research Council of Israel, Vol. IIC, No. 1, p. 97, April 1962.

2. Singer, J., and Eckstein, A., RECENT EXPERIMENTAL STUDIES OF BUCKLING OF CONICAL SHELLS UNDER TORSION AND EXTERNAL PRESSURE, Proceedings of the Fifty Israel Annual Conference on Aviation and Astronautics, p. 135, February 1963.

3. Weingarten, V. I., Morgan, E. J., and Seide, P., FINAL REPORT ON THE DEVELOPMENT OF DESIGN CRITERIA FOR ELASTIC STABILITY OF THIN SHELL STRUCTURES, Space Technology Laboratories, Los Angeles, TR-60-0000-19425, December 1960.

4. Weingarten, V. I., and Seide, P., ELASTIC STABILITY OF THIN WALLED CYLINDRICAL AND CONICAL SHELLS UNDER COMBINED EXTERNAL PRESSURE AND AXIAL COMPRESSION, AIAA Journal, Vol. 3, No. 5, p. 913, May 1965.

5. Magula, A. W., STRUCTURAL TEST-CONICAL HEAD ASSEMBLY - TEST No. 815, North American Aviation, Inc., Missile Development Division, Report MTL 351, July 1954.

6. Westmoreland, R. T., TEST OF MODEL CONICAL BULKHEAD - TEST 1098, North American Aviation, Inc., Missile Development Division, Report MTL 652, May 1956.

7. Homewood, R. H., Brine, A. C., and Johnson, A. E., Jr., BUCKLING INSTABILITY OF MONOCOQUE SHELLS, AVCO Corporation, Research and Advanced Development Division, RAD-TR-9-59-20, August 1959.

8. Ebner, H., and Schnell, W., EINBEULEN VON KREISZYLINDERSCHALEN MIT ABGESTUFTER WANDSTARKE UNDER AUSSENDRUCK, Zeitschrift fur Flugwissenschaften, Vol. 9, Heft 4/5, p. 1943, April 1961.

9. Batdorf, S. B., A SIMPLIFIED METHOD OF ELASTIC STABILITY FOR THIN CYLINDRICAL SHELLS, NACA Report 874, 1947.

10. Seide, Paul, ON THE BUCKLING OF TRUNCATED CONICAL SHELLS UNDER UNIFORM HYDROSTATIC PRESSURE, Proceedings of the IUTAM Symposium on the Theory of Thin Elastic Shells, held at Delft, Holland, August 1959, North-Holland Publishing Company, Amsterdam, 1960, p. 363.

11. Singer, Josef, BUCKLING OF CONICAL SHELLS UNDER AXISYMMETRICAL EXTERNAL PRESSURE, Journal of Mechanical Engineering Science, Vol. 3, No. 4, p. 330, December 1961.

12. Singer, Josef, CORRELATION OF THE CRITICAL PRESSURE OF CONICAL SHELLS WITH THAT OF EQUIVALENT CYLINDRICAL SHELLS, AIAA Journal, Vol. 1 No. 11, p. 2675, November 1963.

13. Sendelbeck, R. L., THE MANUFACTURE OF THIN SHELLS BY THE ELECTRO-FORMING PROCESS, Stanford University, Department of Aeronautics and Astronautics, Stanford, California, SUDAER Report No. 185, April 1964.

14. Niordson, F. I. N., BUCKLING OF CONICAL SHELLS SUBJECTED TO UNIFORM LATERAL PRESSURE, Transaction of the Royal Institute of Technology, Sweden, No. 10, 1947.

15. Mushtari, K. M., and Sachenkov, A. V., STABILITY OF CYLINDRICAL AND CONICAL SHELLS OF CIRCULAR CROSS SECTION, WITH SIMULTANEOUS ACTION OF AXIAL COMPRESSION AND EXTERNAL NORMAL PRESSURE, NACA TM 1433, April 1958 (Original Published in PMM Vol. 18, No. 6, November-December 1954).

16. Seide, Paul, ON THE FREE VIBRATIONS OF SIMPLY SUPPORTED TRUNCATED CONICAL SHELLS, Proceedings of the 7th Israel Annual Conference on Aviation and Astronautics, Israel Journal of Technology, Vol. 3, No. 1, p. 50, February 1965.

17. Sobel, L. H., EFFECTS OF BOUNDARY CONDITIONS ON THE STABILITY OF CYLINDERS SUBJECT TO LATERAL AND AXIAL PRESSURES, AIAA Journal, Vol. 2, No. 8, p. 1437, August 1964.

18. Baruch, M., Harari, O., and Singer, J., EFFECT OF IN-PLANE BOUNDARY CONDITIONS ON THE STABILITY OF CONICAL SHELLS UNDER HYDROSTATIC PRESSURE, Proceedings of the 9th Israel Annual Conference on Aviation and Astronautics, Israel Journal of Technology, Vol. 5, No. 1, p. 12, February 1967.

19. Carlson, R. L., Sendelbeck, R. L., and Hoff, N. J., AN EXPERIMENTAL STUDY OF THE BUCKLING OF COMPLETE SPHERICAL SHELLS, NASA CR-550, August 1966.

20. Horton, W. H., and Durham, S. C., REPEATED BUCKLING OF CIRCULAR CYLINDRICAL SHELLS AND CONICAL FRUSTRA BY AXIAL COMPRESSIVE FORCES, Stanford University, Department of Aeronautics and Astronautics, Stanford, California, SUDAER Report No. 175, November 1963.

APPENDIX I
THE MANUFACTURE OF ELECTROFORMED CONICAL SHELLS

The manufacture of conical shells by the electroforming process is not unique in itself. It is only when one requires a high degree of specimen uniformity that difficulties are presented. Such was the case in this investigation.

In brief outline, the approach and technique used to develop a specimen of high dimensional quality are presented.

Although the electroforming process is well suited to the manufacturing of thin shells, thickness variations often occur. However, since these variations are located at the same places for any number of shells plated under identical conditions, it becomes apparent that this is not a random phenomenon. Consequently, by manipulation of the proper parameters, it should be possible to control such thickness variations.

Of the several techniques considered, the "shaded cathode" method was chosen as the most appropriate. It controls thickness buildup by directing and constricting the natural current distribution on the cathode, which in our case was the mandrel.

A detailed account of the above technique is presented in a paper on "Control of Thickness Variations of Nickel Plate During the Electroforming Process", which is presently being edited for publication. A brief description of this technique follows.

The conical mandrel was located in the plating tank with its small end down and its longitudinal axis in a vertical position. It was slowly rotated about this axis at an approximate speed of 1/8 rpm. The aluminum mandrel was originally plated without any "shading". The plating was removed from the mandrel and its thickness variations were measured and located. It was found that without shading there was considerable buildup at both ends of the shell.

The type of shading first tried was to attach Plexiglas circular plates to both ends. These plates were purposely made with large diameters in order to drastically restrict the current distribution on the mandrel, thereby hopefully causing an extreme "thinning down" of the shell at its ends. This actually occurred; and as a result, the two thickness extremes were established. By reducing the diameter of the flanges, the thickness of the shell at its ends was brought to the desired dimensions. It was also found that for these shading flanges to have an appreciable effect along the entire length of a shell, rather than at its ends only, it was necessary to direct the flanges at some specific angle to the surface being plated. The shading for shells of 30° cone angle took the shape of

a circular apron with an angle of 75° to the mandrel surface (Figure 10). With this kind of shading configuration, shells with longitudinal thickness variations of less than 4 percent were produced.*

Thickness uniformity in the circumferential direction was found to be less than 3 percent of the mean thickness.

With all parameters held constant, it was possible to control the mean thickness of a shell merely by manipulation of the length of plating time involved in the process.

With the present technique, which was worked out for this specific type of shell, it was found that the minimum mean thickness which could be satisfactorily plated was about .0028 inch. However, it is believed that by further development of the technique, considerably thinner specimens of high uniformity may be achieved.

A number of shells have been manufactured in which all the parameters were held reasonably constant; the resulting uniformity of thickness has established a good repeatability record.

The mandrel, or form, over which the nickel was plated was made of aluminum because the nickel-plated shell does not adhere tenaciously to it; consequently, this greatly simplifies the separation problem. This process simply involves heating of the plated mandrel to about 400°F. Since the coefficient of expansion of aluminum is about twice that of nickel, the mating surfaces of the two metals shift relative to each other when heat is applied; and when the small end of the cone is pointed downward, the shell will fall free at some time during the cooling period.

Blemishes, particles of foreign material settling on the plating surface, and plate pitting were all methodically eliminated by techniques usually employed in electroplating.

The three major parameters affecting physical properties of nickel plate which were held reasonably constant during the entire manufacturing program, were: (1) solution pH, (2) solution temperature, (3) current density.

* The instrument used for measuring shell thickness was a dial gage mounted to perform its function most accurately (Figure 11). Its limits of accuracy were determined to be ±.00003 inch.

APPENDIX II
LIST OF PARTS AND PART NUMBERS

PART NO.	PART
SUPPORT STRUCTURE	
1	Out-of-Roundness-Device Counterweight
2	Out-of-Roundness-Device Counterweight Shaft
3	Out-of-Roundness-Device Base Disc
4	Out-of-Roundness-Device Center Block
5	Counterweight Hook
6	Top Support Rod
7	Out-of-Roundness-Device Horizontal Arm
8	Out-of-Roundness-Device Vertical Arm
9	Top Disc
10	Top Support Ring
11	Top Support Ring Bolts
12	Top O-Seal
13	Top Support Disc
14	Top Support Disc Bolt O-Seal
15	Top Support Disc Centering Pin
16	Detachable Rod
17	Bottom Support Bolt Nuts
18	Bottom Support Bolts
19	Bottom Support Ring
20	Bottom O-Seal
21	Base Disc Level Adjuster Screws
22	Base Support Centering Pins
23	Base Plate

PART NO.	PART
24	Base Disc
25	Base Support Disc
26	Deflection Dial Gage
27	Dial Gage Bolt

VACUUM AND PRESSURE MEASURING SYSTEMS

28	Vacuum Storage Tank
29	Vacuum Pump
30	Main System Valve
31	Vertical Mercury Manometer
32	Vacuum Tank Valve
33	Vacuum Pump Valve
34	Flow Control Micro-Valve
35	Incline, Water Manometer
36	Manual Pressure Release Valve
37	Push Button Pressure Release Solenoid Valve

CENTERING DEVICE

38	Hollow Level Ring
39	True Level Plate
40	Pencil Point Indicator
41	Centering Device

COUNTERWEIGHT SYSTEM

42	Ball Bearing Pulleys
43	"Gallows" Structure

PART NO.	PART
44	Nylon String
45	Weight Counter
46	Vertical Support Pipe
47	Vertical Support Pipe Fixing Screws